* 2nd Place Winner 1998 Roon Awards Competition *

Parameters Influencing the Spray Behavior of Waterborne Coatings

Lin-lin Xing and J. Edward Glass†—North Dakota State University*
and
Raymond H. Fernando††—Armstrong World Industries, Inc.

The influence of liquid pressures and orifice diameters on the sprayability of non-Newtonian, waterborne latex coatings, that vary in latex particle size and thickener composition are examined in this study. It is observed that the higher the dynamic uniaxial extensional viscosities (DUEVs, η_e) of the coatings, the larger the Sauter mean diameters (SMDs) of the spray droplets and the broader the droplet size distributions. The shear viscosities at high shear rates and the parameter reflecting shear elasticity, the storage moduli, at low deformation rates do not correlate with the droplet sizes and the distributions observed. In addition to these observations, the Sauter mean diameters of spray droplets decrease with increasing spray pressures and with decreasing orifice diameters; however, with increasing pressures, pulsations in the fluid due to turbulence create areas of high and low droplet density.

The relationship of the SMD to orifice diameters using fan nozzles is defined by the relationship:

$$SMD/d_h = 5.5\,[\sigma\eta_e^4/(\rho_A d_h^3 \Delta P_L^2)]^{0.25} + 2\,[\sigma\rho_L/(\rho_A d_h \Delta P_L)]^{0.25}$$

The experimental results associated with each of these parameters are discussed in the text.

INTRODUCTION

Although the application of coatings by spray has been practiced for over 70 years, the process is still not well understood because of the complexity of the atomization process, differences in the design, size, and operating conditions of the nozzles tested, and variations in the fluid's properties. In airless pressure spray application,[1-3] the coating is forced by a high fluid pump pressure (400-2000 psi) through a very small orifice (0.18-1.2 mm in diameter) causing it to atomize into very fine droplets. The variables influencing the airless spray pattern of Newtonian fluids are the viscosity of the fluid, fluid pressure, nozzle shape and size, and gun-to-surface distance. Usually, the gun is held 12-14 in. from the surface.

For a non-viscous liquid, Rayleigh[4] first predicted that the filament would break up into essentially spherical drops with a uniform diameter D_{AV} for a given orifice diameter, d_n

$$D_{AV} = 1.89\, d_n$$

For a more viscous liquid, Weber[5] used a modified diameter ratio:

$$D_{AV}/d_n = 1.89\,[1 + 3\,We_L^{1/2}/Re_L]^{1/6}$$

The liquid Reynolds (Re) and the liquid Weber (We) numbers (two dimensionless groups), are defined as:

$$Re_L = \rho_L V_j d_n/\eta_L$$

$$We_L = \rho_L V_j^2 d_n/\sigma$$

where: V_j = liquid jet velocity, σ = surface tension,
ρ_L = liquid density, η_L = liquid viscosity
d_n = orifice diameter

The Re number represents the ratio of inertia forces to the viscous force, and the We number represents the ratio of the disruptive aerodynamic forces to the fluid's surface tension.

Presented at the 1998 Annual Meeting of the Federation of Societies for Coatings Technology, on October 15, 1998, in New Orleans, LA.
†Person to whom correspondence should be sent.
*Polymers and Coatings Department, Fargo, ND 58105.
††Research Development Center, Lancaster, PA 17604.

Table 1—The Formulation of Latex Coatings

Material, Supplier	Function	wt%
TiO_2-R900, DuPont	Pigment	17.8
Tamol 731 (25 wt%), Rohm & Haas	Dispersant	0.5
Tergitol 15-S-9, Rohm & Haas	Surfactant	0.25
Ethylene Glycol	Freeze-thaw stabilizer	1.25
Texanol, Eastman Chemical	Coalescing aid	1.25
NDW, Henkel	Antifoaming agent	0.29
Phenyl Mercuric Acetate, Aldrich	Anti-fungus agent	0.0375
Latex (46 wt%), Rohm and Haas and S.C. Johnson	Binder	38.5
Water & thickener		40.2
Total		**100.0**

Ohnesorge[6] also observed that jet stability is a function of Reynolds number (i.e., jet dissipation is a function of liquid viscosity, density, surface tension, and nozzle size). He expressed the mechanism of liquid breakup in three stages, each stage characterized by the magnitude of the ratio of the (Weber)$^{0.5}$/Reynolds dimensionless numbers, reflected in the ratio of viscous to surface tension forces.

$$We^{1/2}/Re = \eta_L/(\rho_L \sigma d_n)^{1/2}$$

In this text we will attempt to develop a relationship in terms of the properties of a coating formulation (η_L, ρ_L, and σ) without reducing it to a dimensionless number.

From an experimental viewpoint there has been only one systematic study of fluid properties across the spectrum of nozzles and application processes. Atomizer types, atomizer geometries, liquid physical properties (surface tension and viscosity), and operational settings have been examined,[7-10] that included air, airless,[7] rotary atomizers,[10] and electrostatic spray[9] equipment. In the first of these studies, Wang and Lefebvre[11] examined the spray process in a hollow-cone nozzle. Diesel oil and water were chosen to provide the variation in surface tension and mixtures of diesel oil and liquid polybutene provided variations in viscosity.

Lefebvre's group also studied[7] the effect of operating conditions and liquid properties on drop sizes and distributions produced by a fan-airless spray atomizer. The fluids employed were water, water/glycerine mixtures, silicone oils, and an unspecified commercial enamel coating. The following equation describes their observations:

$$SMD/d_h = 2.83\,(\sigma\mu_L^2/\rho_A\, d_h^3\, \Delta P_L^2)^{0.25} + 0.26\,(\sigma\rho_L/\rho_A d_H\, \Delta P_L)^{0.25}$$

where: SMD = Sauter mean diameter, m
d_h = hydraulic mean diameter of nozzle orifice, m
σ = surface tension, N/m
μ_L = absolute viscosity of liquid, Ns/m^2
ρ_A = density of air, kg/m^3
ρ_L = density of liquid, kg/m^3
ΔP_L = nozzle injection pressure differential, Pa

This equation is unsuitable for liquids which combine high surface tension (>73 mN/m) with very high viscosity (100*10^{-6} m^2/s, or 100 cst). The authors explained that when a high surface tension is accompanied by an abnormally high viscosity, a change in the mode of sheet disintegration into drops occurs. These studies and other investigations of possible peripheral interest to the spray application of coatings have been reviewed in a prior report of our studies.[12] The studies described in all of the above investigations have been on Newtonian fluids.

In spray applications of real coating systems, which are generally non-Newtonian,[13,14] it is common to relate the sprayability of a coating to its viscosity at high shear rates. This was also true in early roll applied coatings that related viscosities at high shear rates to spatter[15]; however, in a more detailed examination of the misting behavior of roll applied coatings,[16,17] spatter was clearly related to dynamic uniaxial extensional viscosities (DUEVs, η_e). As Strivens[18] has noted, studies of this nature have been ignored, and most who review these areas pretend that coatings do not exhibit viscoelastic behavior. Non-Newtonian behavior occurs in industrial coatings used in spray studies,[13,14] and most waterborne coatings exhibit non-Newtonian flow. The objective of this study is to examine the interaction of spray process conditions (i.e., liquid pressures and orifice diameters) on the sprayability of non-Newtonian, waterborne latex coatings varying in latex particle size and thickener composition. The rheological responses of the coating systems are compared with the misting behaviors and droplet size distributions observed in the patterns obtained from airless spray fan nozzles. It was implied[12] based on previous roll application studies[16] that the lack of sprayability of hydroxyethyl cellulose and poly(oxyethylene) coatings was related to DUEVs of these thickeners in aqueous solutions. In this article we get "real" and quantify the relationship through the use of airless sprays at higher application pressures.

EXPERIMENTAL SECTION

Formulation of Latex Coatings

The formulations (*Table* 1) contain an acrylic latex (477 nm or 68 nm particle size) and TiO_2 (28% NVV, 20% PVC). The amounts of the thickeners used in the final formulation are given in *Table* 2.

Airless Spray Process

Airless spray applications were conducted at different fluid pump pressures (100, 400, 900, 1800 psi) using a Wagner 505 high performance airless spray system. Reversible fan spray tips were used (*Table* 3).

Measurement of Droplet Size and Their Distribution in Spray Coatings

Collection of Spray Droplets: The spray droplets were collected on a special black paperboard which was

Table 2—Characterization and Amount of the Thickeners Used in the Latex Coatings

Thickener	Mv	Wt% Added to 477 nm Latex	Wt% Added to 68 nm Latex
High Wt. POE, (poly (ethylene oxide))	$6.0* 10^6$	0.001	0.001
		0.005	0.005
		0.02	0.02
		0.05	0.05
		0.1	0.1
High MWt., HEC (hydroxyethyl cellulose)	$9.5* 10^5$	0.25	0.43
Low MWt., HEC	$6.8* 10^4$	1.2	1.1 (phase separated)
HEUR–60[a]	$2.9* 10^4$	0.25	0.53
HEUR–40[b]	$2.7* 10^4$	0.24	0.79
HEUR–45[c]	$2.5* 10^4$	1.0	1.7

(a-c) The synthesis and characterization of model Hydrophobically-modified, Ethoxylated Urethanes (HEUR) thickeners is a laborious task and spray studies demand significant amount of materials. We chose to use these commercial materials from King Industries, and our assessment of $C_{18}H_{37}$–, $C_{14}H_{29}$–, and C_6H_{13} terminal sizes from these respective materials is an approximation based on our previous studies of model HEURs,[19] not a disclosure of King Industries.

placed behind a plate having a narrow slit (*Figure* 1). When the flow of the spray became stable, the plate having a narrow slit was moved upward at a constant speed so that the droplet density on the black paperboard was controlled in the range of 30-80 numbers/cm^2. The air movement generated from moving the plate is negligible compared to the air movement generated from the fast moving droplets. Therefore, there is no additional air force for additional breakup when the droplets go through the slit. The collection distance between the spray nozzle and the slit was fixed at 30.5 cm. The particle size distribution data were calculated through statistical analysis. It is important for an image analysis instrument to be able to identify the individual droplet in order to obtain reliable droplet size and size distribution data. We controlled the size of the slit to control the droplet density on the substrate within the range of 30-80 numbers/cm^2 in order to avoid the overlapping of droplets on the substrate.

Sizing of Droplet Size and Distribution: Stain sizes of sprayed droplets were analyzed using Optimas image analysis software (Optimas Corporation, Version 5.10, Media Cybernetics, L.P., Bothell, WA 98011; http://www.optimas.com).

Sauter Mean Diameter of Droplets: This is defined as the diameter of a droplet whose ratio of volume to surface area is equal to that of the entire sample.

$$SMD\ (D_{vs}) = \Sigma(N_i D_i^3) / \Sigma(N_i D_i^2)$$

where: N_i is the number of droplets having a D_i diameter. The advantage of using Sauter Mean Diameters is that they permit calculation of the total surface area of an atomized volume of fluid.

The SMD can be calculated from the transformation:

$$\ln D_{vs} = \ln D_{GM} + 2.5* \ln^2 S_G$$

where: $D_{GM} = D_{50\%}$ and $S_G = D_{84.14\%} / D_{50\%}$

$D_{50\%}$ and $D_{84.14\%}$ can be obtained from the log-Normal Probability plot of droplet sizes (from a statistic program, Minitab 10.5). A typical log-Normal Probability plot of droplet sizes is shown in *Figure* 2. For additional details on this type of analysis see *Spray Drying, An Introduction to Principles*.[20]

We assumed that the "splattered" particles have circular shapes. The surface tensions of the liquids range from 35-45 dyne/cm and with the small sizes of the spray drops they should remain circular. This was observed in most cases in the imaging analysis instrument. We did not convert the stained particle diameter to an "in flight" particle diameter. These studies are in progress using particle image velocimetry laser equipment and will be reported in time.

The size distribution of droplets can be represented by a coefficient of variation that is equal to the ratio of the standard deviation, S, of droplet sizes to the mean diameter of the droplets, D_{AV}. The smaller the coefficient of variation (CV), the narrower the size distribution:

$$\text{Coefficient of Variation} = S/D_{AV}$$

where D_{AV} is the number average diameter of particle. D_{50} is calculated from the log-Normal probability plot. If

Table 3—Spray Tips Used in Airless-Spray Application

Orifice Size (in.)	Orifice Size (mm)	Flow Rate[a] (GPM)[b]	Fan Width[c] (mm)
0.015	0.381	0.23	203 - 254
0.013	0.330	0.17	203 - 254
0.011	0.279	0.12	203 - 254

(a) Flow rate established with water at 2000 psi (138 bar) at the tip.
(b) GPM: gallons per minute.
(c) These data were supplied by the manufacturer. The width as a function of the distance was not specified, but is assumed that the target is 304 to 355 mm.

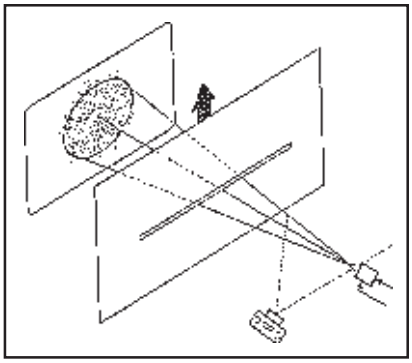

Figure 1—Illustration of droplet collection for spray process.

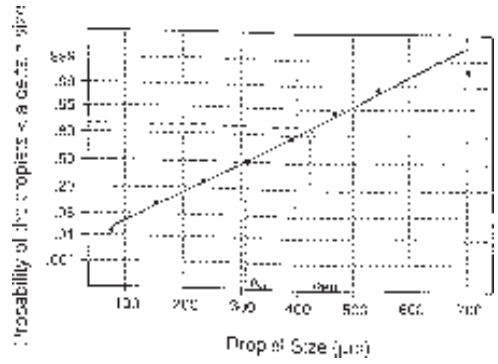

Figure 2—A log-normal probability of droplet sizes.

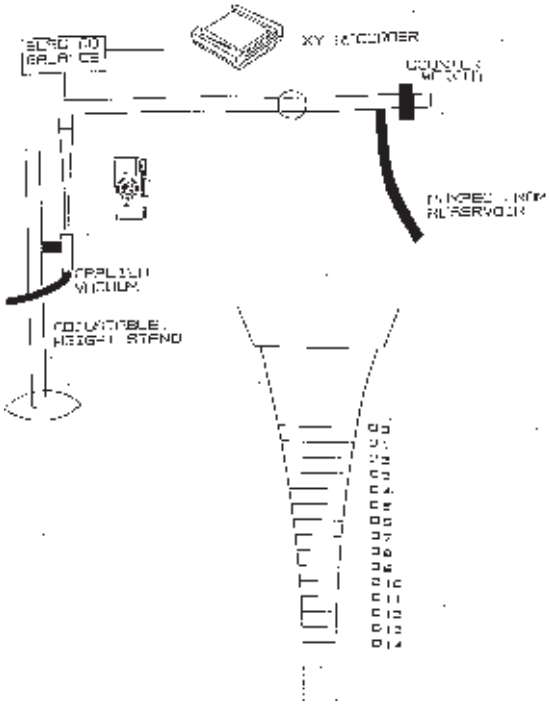

Figure 3—The measurement of Dynamic Uniaxial Extensional Viscosities (DUEVs) through a fiber extension method.

data points provide a straight line, D_{AV} should be equal to D_{50}.

Rheology Measurements

Steady State Shear Flow and Oscillatory Flow Profiles: The steady state shear flow under 0-1000 s^{-1} shear rate (0-597 Pa shear stress) and oscillatory flow profiles (linear region, displacement = 2.5* 10^{-4} ~ 3.0 * 10^{-4} rad) were measured with a Carri-Med CSL 100 controlled stress rheometer (Cleveland, OH) using a cone and plate (cone angle = 2°, with 4 cm diameter) or a double-concentric cylinder geometry. High shear rate viscosities (12,000 s^{-1}) were measured with an ICI cone and plate viscometer. All the measurements were performed at 25°C.

Measurement of Dynamic Uniaxial Extensional Viscosities (DUEVs, η_e)**:** Dynamic Uniaxial Extensional Viscosities were measured via a fiber extension method. The general equipment is illustrated in *Figure* 3. A pulse-free, magnetic-drive gear pump (Micopump Co., IL) was used to pump fluid; an electrobalance (Cahn Model 7000) attached to a XY recorder (Hewlett-Packard) measured the resistance force from the fiber. The force measured by electrobalance is the resistance force of the fluid to the extensional flow, and therefore taken under the flow condition. The force measured is recorded on an XY recorder. When a vacuum suction force is suddenly applied, the extensional flow is not uniform and this is reflected by variations on the recorder. When the varia-

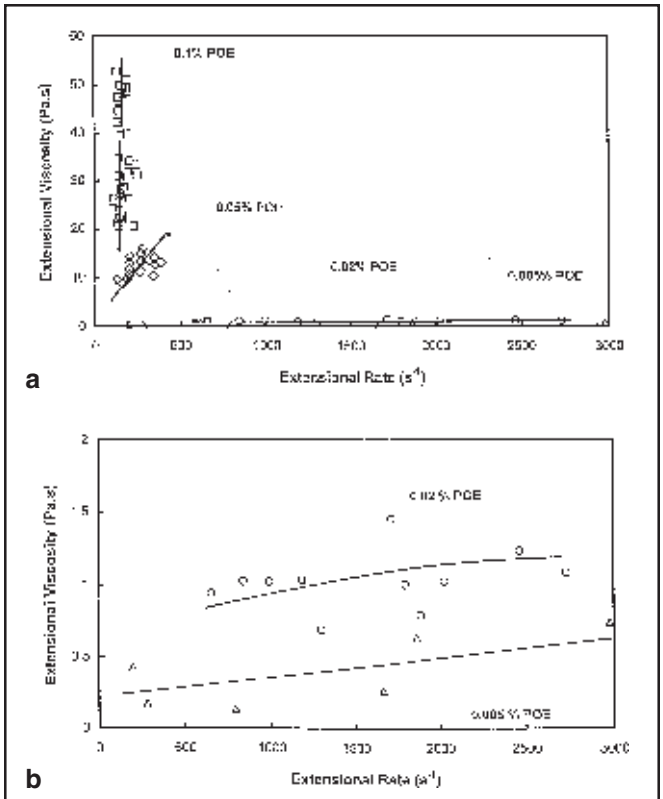

*Figure 4—The DUEV of 68 nm latex coatings—thickener POE wt% (Mv = 6.0*10⁶).*

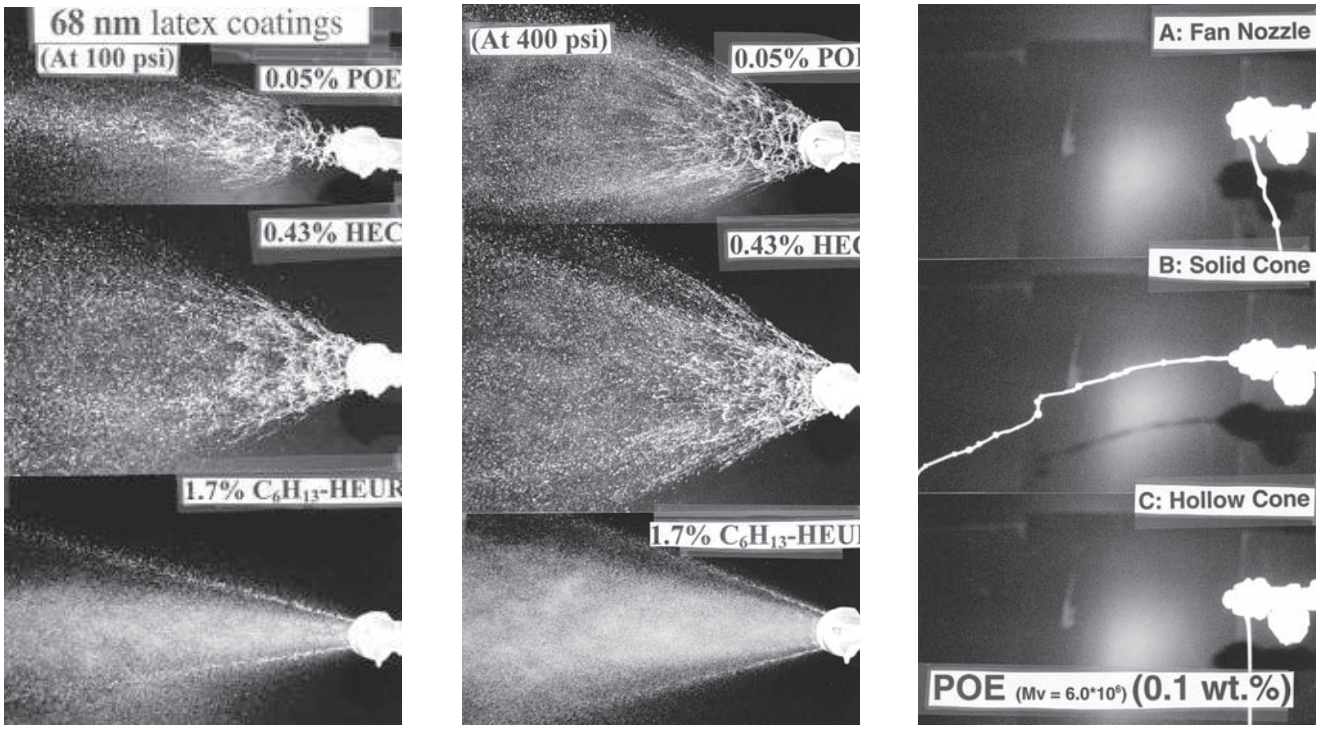

*Figure 5—The air spray patterns of 68 nm latex coatings—thickener POE wt% (Mv = 6.0*10⁶) through fan, solid cone, and hollow cone nozzles.*

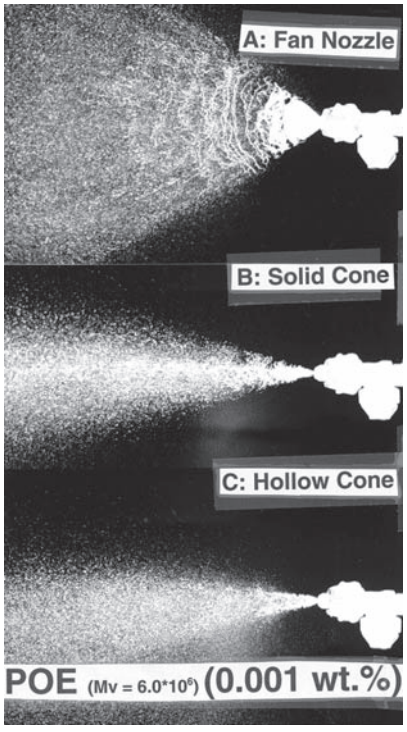

Figure 6—The air spray pattern of 68 nm latex coatings—0.001 wt% POE thickener (Mv = 6.0 10⁶) through fan, solid cone, and hollow nozzles.*

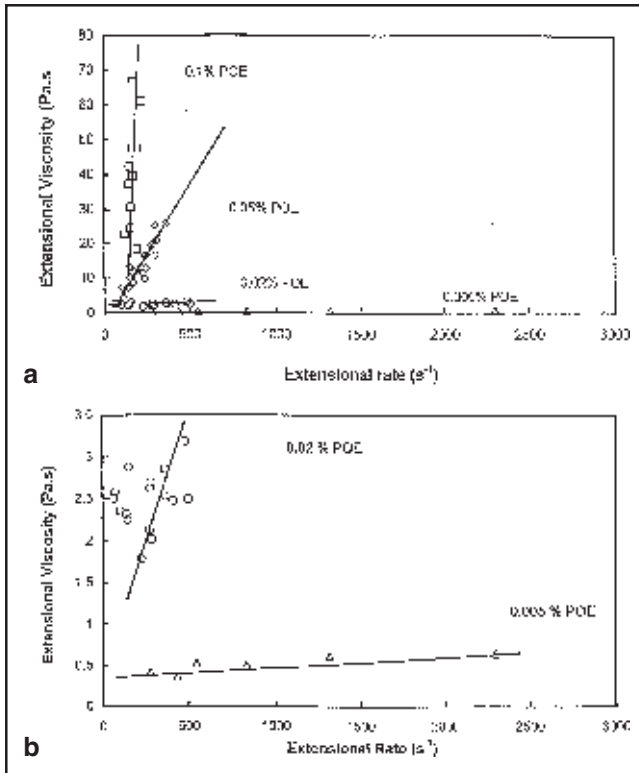

Figure 7—The extensional viscosity of 477 nm latex coating—thickener POE wt% (Mv = 6.0`10⁶).*

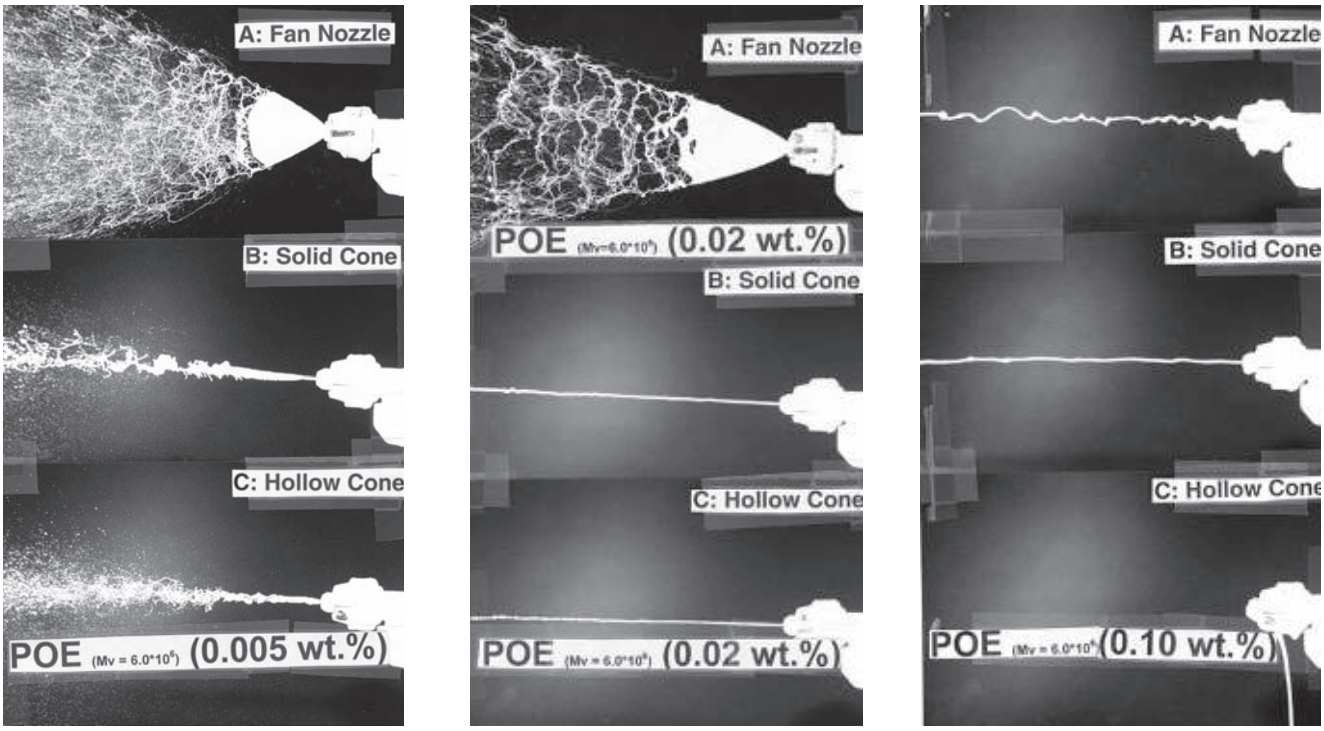

*Figure 8—The air spray patterns of 477 nm latex coatings—thickener POE wt% (Mv = 6.0*10^5).*

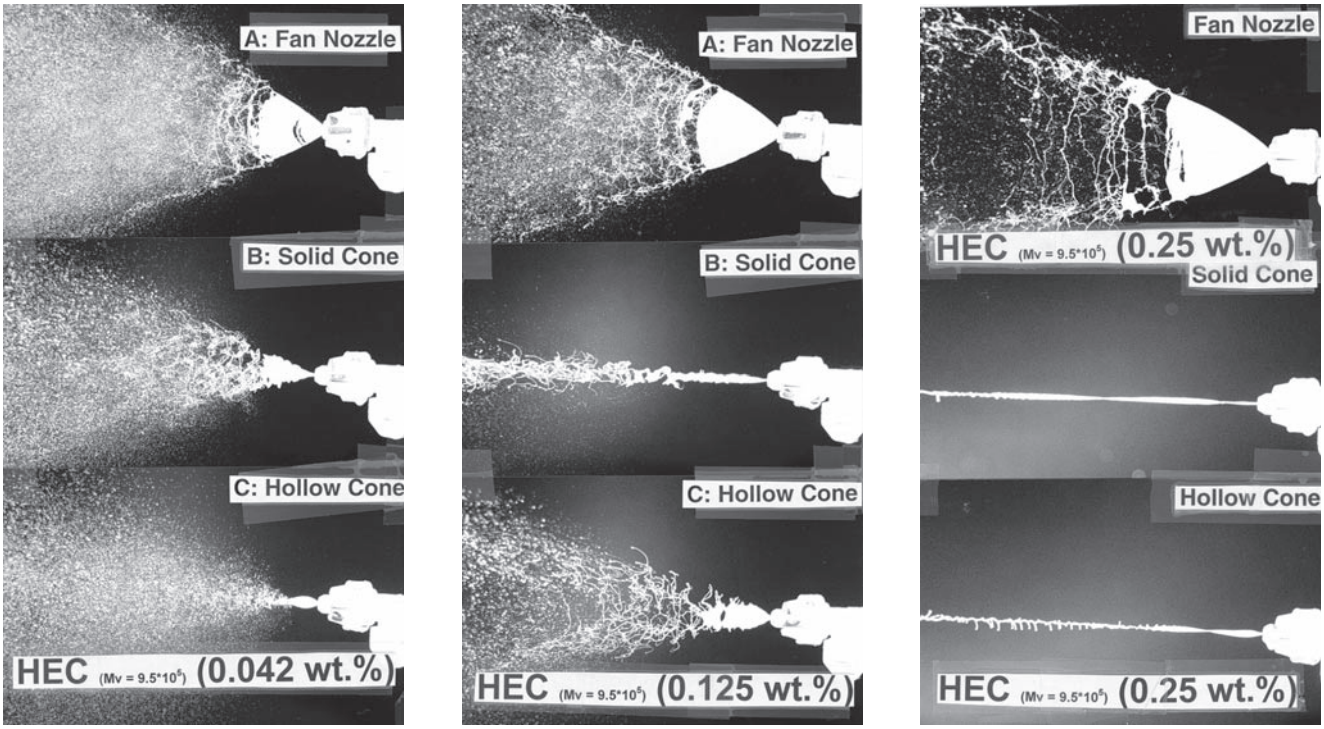

*Figure 9—The air spray patterns of 477 nm latex`coatings—thickener POE wt% (Mv=9.5*10^5) through fan, solid cone, and hollow cone nozzles.*

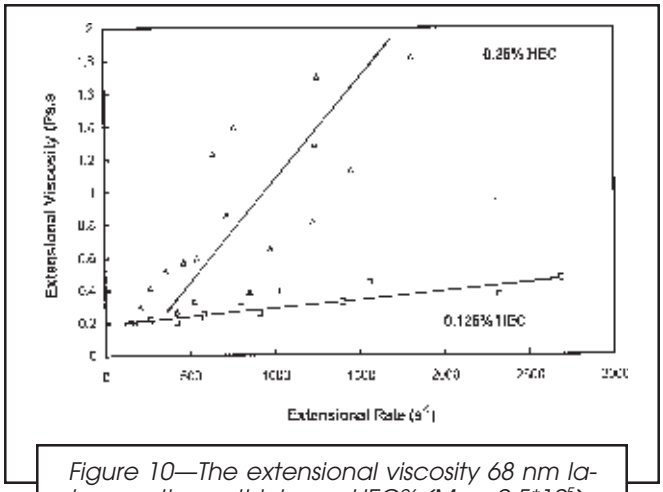

*Figure 10—The extensional viscosity 68 nm latex coatings—thickener HEC% (Mv = 9.5*10^6)*

tions in response subside to a constant value, we assume that a uniform extensional flow is reached and the extended fluid fiber is photographed. A stand for varying the length of the fiber was used in the measurements; a Minolta 35 mm camera was used to photograph the fluid fibers. A vacuum provided the applied force to the fiber, a mercury manometer was used to measure external pressures applied to the fiber.

Experimental Procedure: The fluid is pumped from a reservoir to the nozzle. The fluid is extruded through a nozzle having a diameter of 2.54 mm and the suction is applied to the fiber through a diameter nozzle of 1.0 mm. The resistance of the fluid under extension is recorded by an electrobalance attached to an XY recorder. Three pictures were taken when the balance gave a uniform reading. The force is marked at the instant the picture is taken. The length and radii are measured with a Nikon Projector. Fiber diameters from the photograph are taken at equally spaced intervals. The lengths and radii of fibers are taken at least one diameter in distance from the exit nozzle to avoid any die swell effects. The mass flow rate of a fluid is obtained by collecting the fluid leaving the top nozzle over a period of time. These parameters are then used in the calculation of extensional viscosity. The equations are listed as follows:

$$\varepsilon = (V_{i+1} - V_{i-1}) \,/\, (X_{i+1} - X_{i-1})$$

$$V_i = 4\,Q \,/\, (\rho \pi D i^2)$$

$$(\tau_{xx} - \tau\ )_{i+1} = V_{i+1}\,(\tau_{xx} - \tau_{zz})_i \,/\, Vi - \rho\sigma\pi^*\,(D_{i+1} - D_i) \,/\, 2Q + \rho\,(V_{i+1} - V_i)$$

$$- 0.5^*\,\rho g\,(1/V_{i+1} + 1/V_i)\,(X_{i+1} - X_{i-1})]$$

$$(\tau_{xx} - \tau_{zz})_0 = 4\,F_{ext} \,/\, \pi D_0^2$$

$$\eta_i = (\tau_{xx} - \tau_{zz})_i \,/\, \varepsilon_i$$

where: V = axial velocity
Q = mass flow rate
ρ = density of fluid
D = diameter of fiber
F_{ext} = force detected by electrobalance
X = axial distance
g = force of gravity
σ = surface tension
ε = extension rate
$(\tau_{xx} - \tau_{zz})$ = extensional stress
η_e = dynamic uniaxial extensional viscosity

RESULTS AND DISCUSSION

In our prior study of the influence of formulation components on the spatter behavior of roll applied latex coatings,[16] high and low molecular weight hydroxyethyl cellulose (HEC) and high molecular weight poly(oxyethylene) (POE) were studied in coatings containing a large, broad size distribution, vinyl acetate/butyl acrylate latex. These same thickeners were chosen for this National Science Foundation study because they provide a unique complex fluid that permits clear delineation between shear viscosities at high shear rates and dynamic uniaxial extensional viscosities. They are utilized in this study using a 477 nm and 68 nm all-acrylic latices. The latices studied come with significant variations in free surfactant (the smallest particle size latex will contain the greatest amount of surfactant).[21] HEC and POE were, therefore, the first thickeners examined because they are insensitive to the variation in surfactant concentration. However, the high molecular weight HEC and POE formulations were not sprayable* in the prior

*A Fann nozzle of 73 mm was applied with an air pressure of 55 psi and fluid pressure of 15-20 psia.

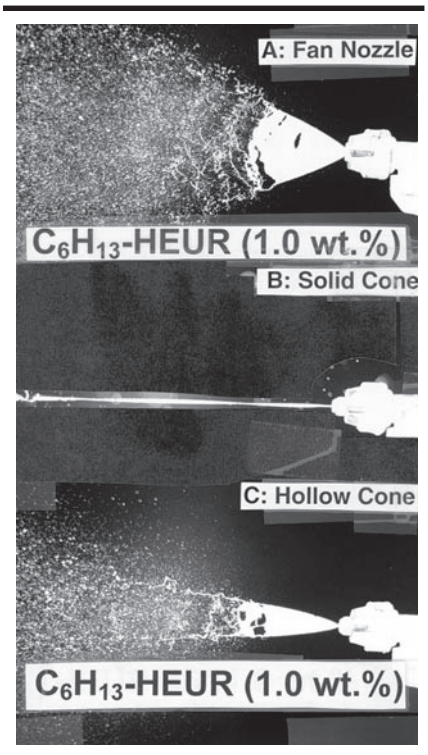

Figure 11—The air spray patterns of 477 nm latex coatings—1.0 wt% C_6H_{13}–HEUR thickener (Mv = 2.5 10^4) through fan, solid cone, and hollow cone nozzles.*

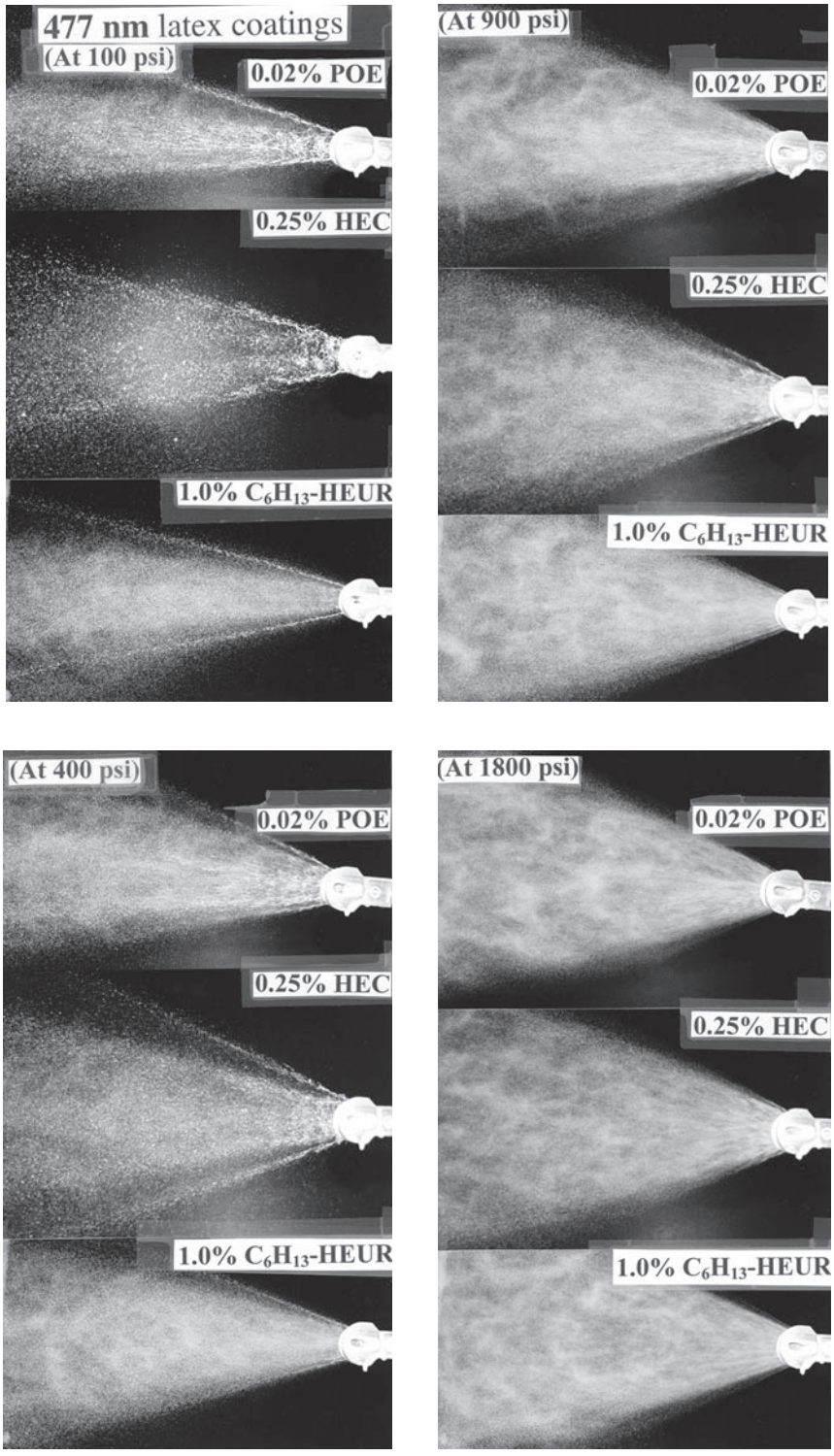

*Figure 12—The airless spray patterns of 477 nm latex coatings—thickeners C_6H_{13}–HEUR (Mv = 2.5*10^4); HEC (Mv = 9.5*10^5); POE (Mv = 6.0* 10^6) through a fan nozzle. Liquid pressures; 100 psi to 1800 psi.*

air spray studies[12]; consistent with our prior roll application studies.[16] When the thickeners were decreased in concentration, the formulations were more sprayable, but the DUEVs of the formulations dropped below detectable limits. We approach the problem in this study by spraying at pressures between 100 to 1800 psi, in airless sprays using fan nozzles. It was expected, just on the commonality of the low amounts required to obtain a given Kreb Unit KU coating for both the large hydrophobe, $C_{16}H_{33}$-HEUR and for the high molecular weight HEC, and on the high shear thinning behavior of both formulations, that the large hydrophobe, $C_{16}H_{33}$–HEUR would not promote a good spray mist. It also was expected that the small hydrophobe, C_6H_{13}–HEUR, with its commonality with the low molecular weight HEC (i.e., the large amount required to attain KU value and the close to Newtonian flow behavior of the formulations), would exhibit good misting behavior. The fact that the opposite spray behavior occurred in both HEUR thickened formulations was one of the more significant observations in the previous study.[12]

The objective of this study is to examine the interaction of spray process conditions (i.e., liquid pressures and orifice diameters) on the sprayability of non-Newtonian, waterborne latex coatings varying in latex particle size and thickener composition. The rheological responses of the coating systems are compared with the misting behaviors and droplet size distributions observed in the patterns obtained from airless spray fan nozzles. It was implied[12] based on previous roll application studies[16] that the lack of sprayability of hydroxyethyl cellulose and poly(oxyethylene) coatings was related to DUEVs of these thickeners in aqueous solutions. We quantify the relationship in coating formulations in this study.

Visualization of the importance of the role of DUEVs in the misting of spray applied coatings is most easily seen in formulations thickened with high molecular weight POE, a water-soluble polymer known for its ability to promote high DUEVs and drag reduction, while contributing little to shear viscosities under deformation. Four formulations containing a 68 nm acrylic latex were prepared with POE concentrations of 0.1, 0.05, 0.02, and 0.005 wt%, respectively. The DUEVs of these formulations were measured (*Figures* 4a and b);

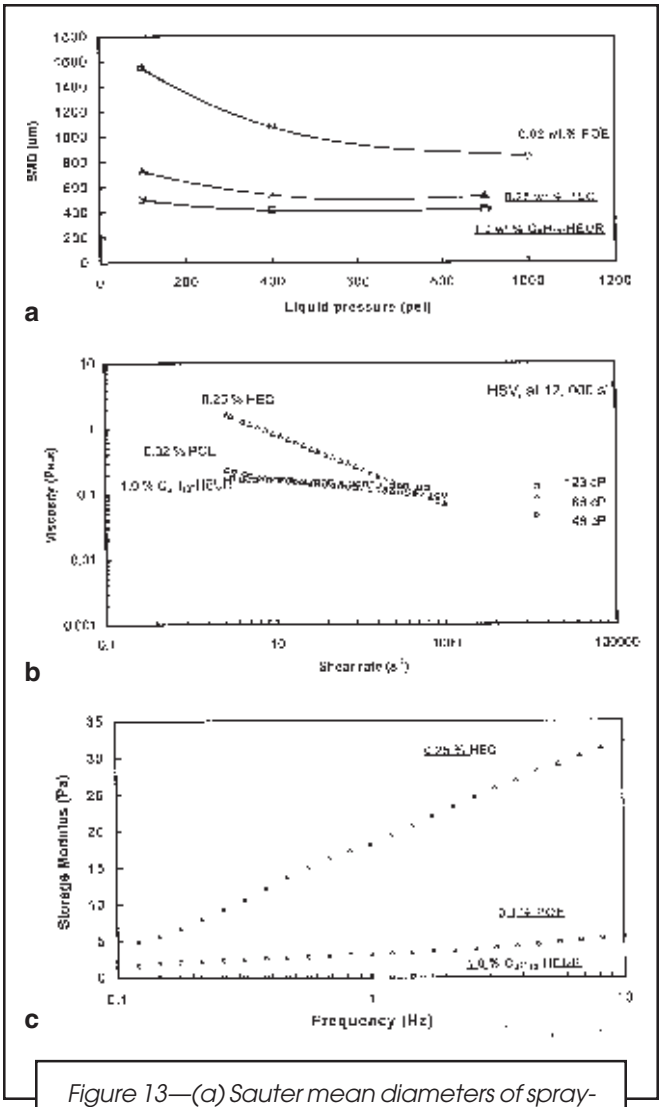

*Figure 13—(a) Sauter mean diameters of spraying droplet size for 477 nm latex coatings—thickeners C_6H_{13}–HEUR (Mv = 2.5*10⁴); HEC (Mv = 9.5*10⁵); POE (Mv = 6.0*10⁶) through airless spray with a fan nozzle.*

*(b)—The shear viscosity of 477 nm latex coatings—thickeners C_6H_{13}–HEUR (Mv = 2.5*10⁴); HEC (Mv = 9.5*10⁵); POE (Mv = 6.0*10⁶).*

*(c)—The storage modulus of 477 nm latex coatings—thickeners C_6H_{13}–HEUR (Mv = 2.5*10⁴); HEC (Mv = 9.5*10⁵); POE (Mv = 6.0*10⁶).*

Symbols (○) 0.02 wt% POE; (Δ) 0.25 wt% HEC; (❑) 1.0 wt% C_6H_{13}-HEUR.

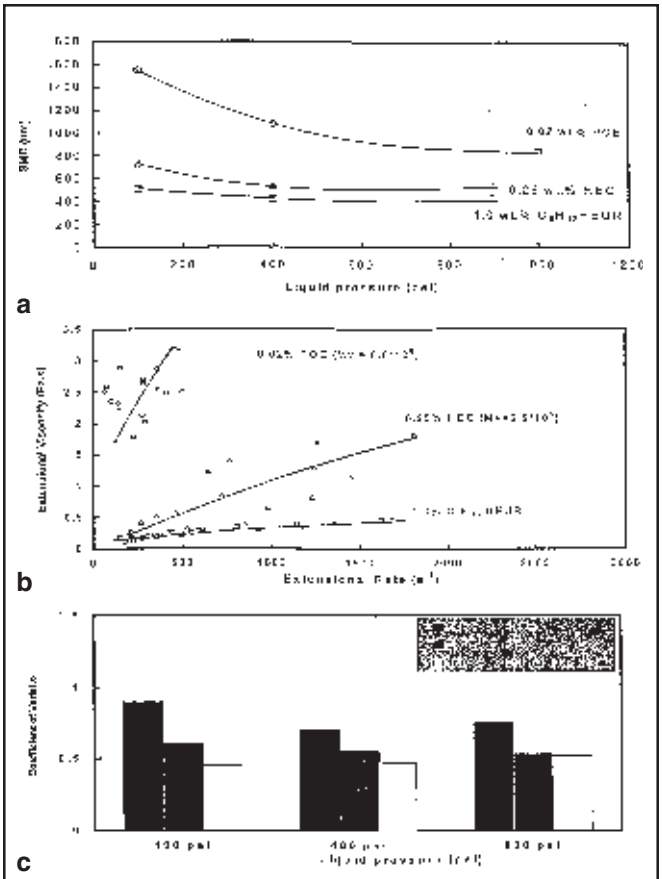

Figure 14—(a) Sauter mean diameters of spraying droplet size for 477 nm latex coatings—thickeners. Symbols (○) 0.02 wt% POE; (Δ) 0.25 wt% HEC; (❑) 1.0 wt% C_6H_{13}-HEUR.

(b) Extensional viscosity of 477 nm latex coatings—thickeners. Symbols (○) 0.02 wt% POE; (Δ) 0.25 wt% HEC; (❑) 1.0 wt% C_6H_{13}-HEUR.

(c)—Droplet size distribution for 477 nm latex coatings—thickeners.

those containing 0.1 and 0.005 wt% POE were not sprayable from any of the nozzle geometries considered in air spray (air pressure 55 psi). This is also true with the 0.005 wt% POE formulation (*Figure* 5) but significant deviation between fan and cone nozzles are observed. The shark skin and irregular appearance observed in the fluid released from the cone nozzles and noted in the extrusions of polyolefins,[22] suggests that the flow pattern from cone nozzles is a biaxial extensional deformation rather than as uniaxial deformation. That is beyond the scope of this paper and will be neglected in this manuscript. More acceptable spray behavior is observed in the formulation when the POE is reduced still further to a 0.001 wt% concentration (*Figure* 6) but measurement of this formulation's DUEVs is beyond the sensitivity level of our measuring device. In parallel studies, replacing the 68 nm latex with the larger 477 nm binder gave similar trends in DUEVs responses (*Figure* 7) and spray patterns (*Figure* 8).

In parallel studies of the high molecular weight HEC thickened formulations containing the 477 nm latex, similar observations in spray behavior (*Figure* 9) and in DUEVs (*Figure* 10) are made. In the last of the three coating thickener formulations that did not spray well (those thickened with the small hydrophobe, C_6H_{13}–HEUR, that exhibited the lowest DUEVs at 1.0 wt% relative to the POE and HEC formulations) the most notable difference in sprayability between the solid and hollow cone nozzles (*Figure* 11) is observed. With these data in hand we set forth to quantify the relations of DUEVs with the spray behavior of these non-sprayable formulations in air spray 55 psi pressure applications by

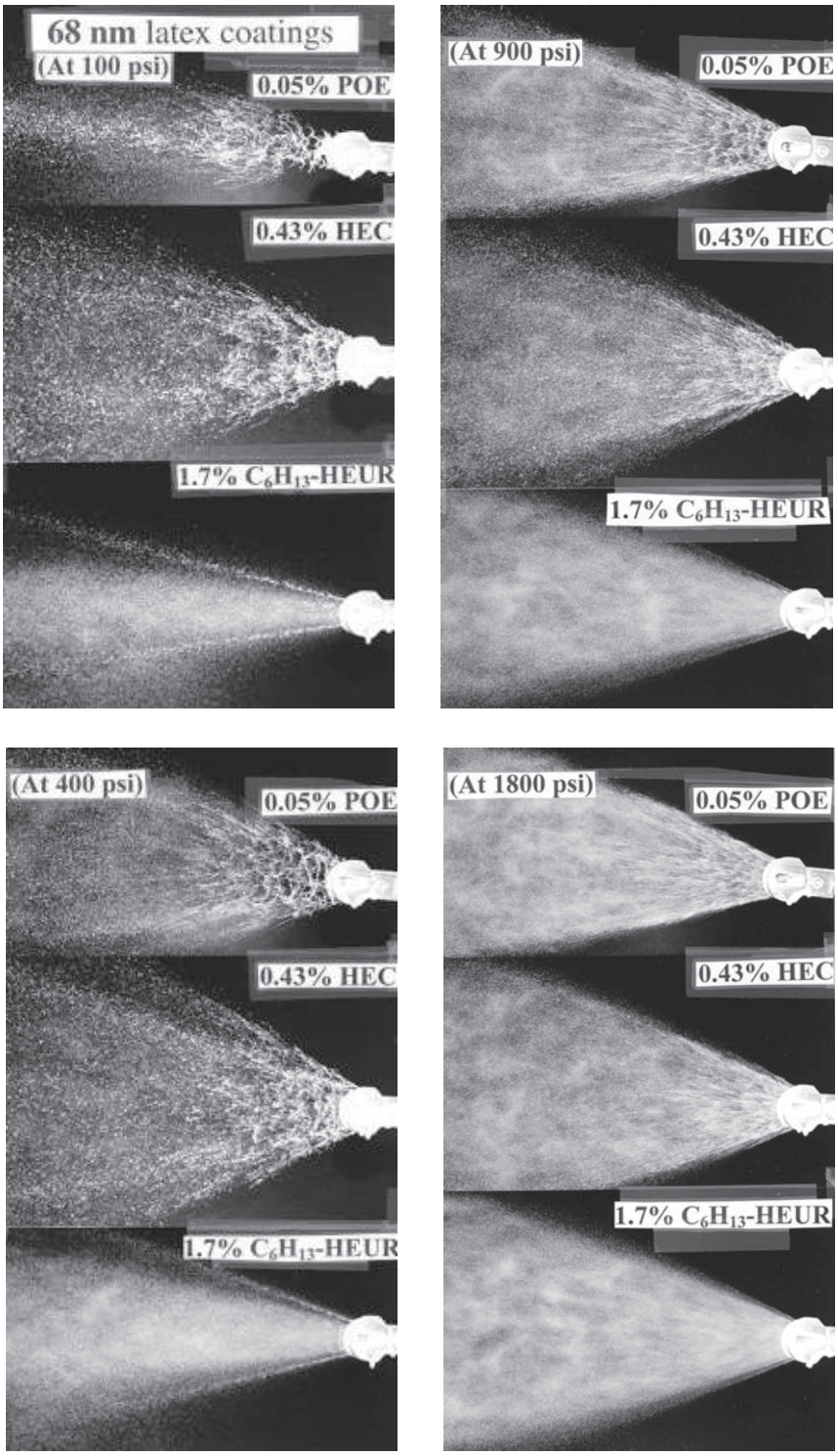

*Figure 15—The airless spray patterns of 68 nm latex coatings—POE wt% (Mv = 6.0*10⁶) through a fan nozzle. Liquid pressures: A, 100 to 400 psi; B, 900 to 1800 psi.*

increasing the application pressures in airless spray using fan nozzles.

The difference in sprayability between the 55 psi and 100 psi patterns is dramatic (compare appropriate photos in *Figures* 8, 9, 11, and 12). As the application pressure increased from 100 to 1800 psi, the visual differences in the sprayability (*Figure* 12) are less notable. In high speed laser particle image velocimetry of industrial automotive coatings, pulsation in the flow patterns are observed with increasing application pressure.[23]

The droplet collection for Sauter Median Diameter measurements (described in the Experimental Section) is done at a distance of 12 in. from the spray nozzles. The Sauter Mean Diameters (SMDs) decrease with increasing liquid pressure for the three 477 nm latex coatings thickened with the different thickeners (*Figure* 13a). The SMD of spray droplets with the 477 nm latex coating containing 0.02% POE is highest among the three latex coatings. The SMD do not correlate with the viscosity dependence on shear rate (*Figure* 13b) or with the elastic function (storage moduli) associated with shear deformations (*Figure* 13c). The SMD data reproduced in *Figure* 14a do correlate with DUEV data (*Figure* 14b). The particle size distributions, reflected in the Coefficient of Variation (CV) data (*Figure* 14c), also demonstrated a general correlation with the relative DUEV data. At higher pressures the pulsation phenomena have to influence the latter analysis. Similar observations were made with the larger 68 nm latex (*Figure* 15).

The differences in the pulsation phenomena with decreasing DUEV are highlighted with the small particle latex thickened with decreasing amounts of POE, specifically at 0.005 wt% POE thickened coatings at 100 and 400 psi (*Figure* 16a) and at 900 and 1800 psi (*Figure* 16b). Again the SMD data (*Figure* 16a) do not correlate with the viscosity dependence on shear rate (*Figure* 16b), but there is a general relationship to the DUEV data (*Figure* 16c), which also show a general relationship with the particle size distribution (CV) data (*Figure* 16d).

The Effect of Orifice Diameters on SMDs of Spray Droplets

For different latex coatings using different thickeners, SMDs decrease in all systems with decreasing orifice

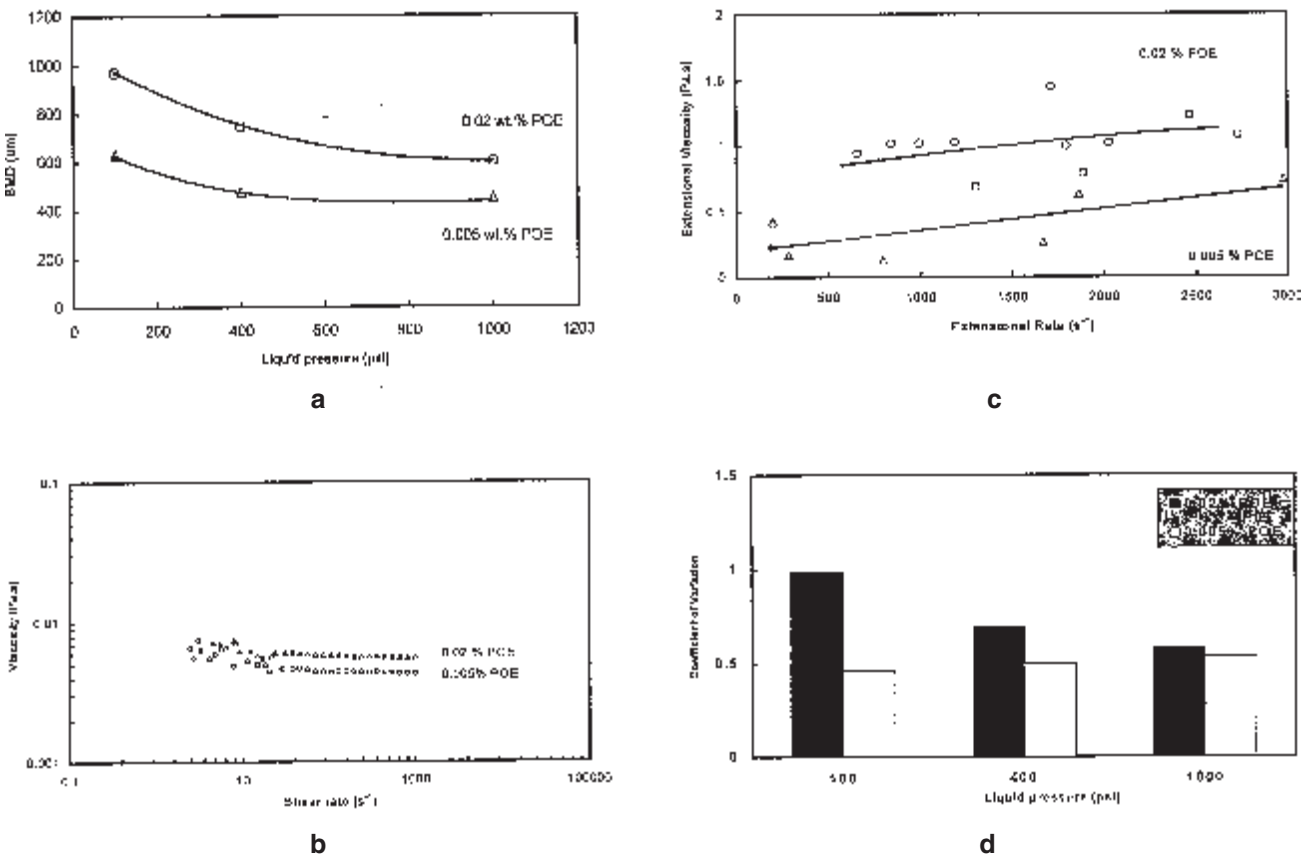

*Figure 16—(a) Sauter mean diameters of spraying droplet size for 68 nm latex coatings—POE % (Mv = 6.0*10⁶).*
*(b) Shear viscosity of 68 nm latex coatings—POE % (Mv = 6.0*10⁶).*
*(c)—Extensional viscosity of 68 nm latex coatings—POE % (Mv = 6.0*10⁶). S*
*(d)—Droplet size distribution for 68 nm latex coatings—POE % (Mv = 6.0*10⁶).*

Symbols (❍) 0.02 wt% POE; (Δ) 0.005 wt% POE.

diameters (examples are illustrated in *Figure* 17). Usually, the smaller the orifice diameter, the lower the flow rate (*Table* 3, i.e., lower amount of fluid existed at the nozzle). At the same fluid pressure, more turbulent flow and higher droplet velocities are achieved with the smaller orifice diameter (i.e., the same aerodynamic force applied to a less amount of coating). Hence, the spray sheet can be broken into finer droplet size with a smaller orifice diameter.

Derivation of Parameter Dependent Equation for Latex Coatings Sprayed by Airless Equipment Through Fan Nozzles

Most waterborne coatings exhibit non-Newtonian flow, and the viscoelastic behavior dominates their flow process behavior. In the studies described previously clearly the viscosities at high and low shear rates do not influence the SMD or size distribution (CV) of the spray droplets. Several linear relationships with the coatings DUEVs are illustrated in *Figures* 18a-d. The dynamic surface tensions of the coatings formulations studied are illustrated in *Figure* 19; noting differences in viscosity on such measurements there is essentially no difference among the data. The densities of these formulations (measured with a Mettler/Paar DMA instrument) did not change with thickener and latex variations. After examining the three important variables in atomization process, such as fluid viscosities, fluid pressure, and orifice diameters, the values of A' and B' are correlated to 5.5 and 2.0 respectively from the experimental data.

The final results of this investigation are surmised in the following equation:

$$SMD/d_h = A' [\sigma\eta_e^4/(\rho_A d_h^3 \Delta P_L^2)]^{0.25} + B' [\sigma\rho_L/\rho_A d_h \Delta P_L)]^{0.25}$$

where:

SMD = Sauter mean diameter of spraying droplets
σ = surface tension of latex coatings
η_e = extensional viscosity of latex coatings
ρ_A = density of air
ρ_L = density of latex coatings
d_h = orifice diameter
ΔP_L = nozzle injection pressure differential

This relationship is illustrated in *Figure* 20. The Sauter mean diameters of spraying droplets for airless spray

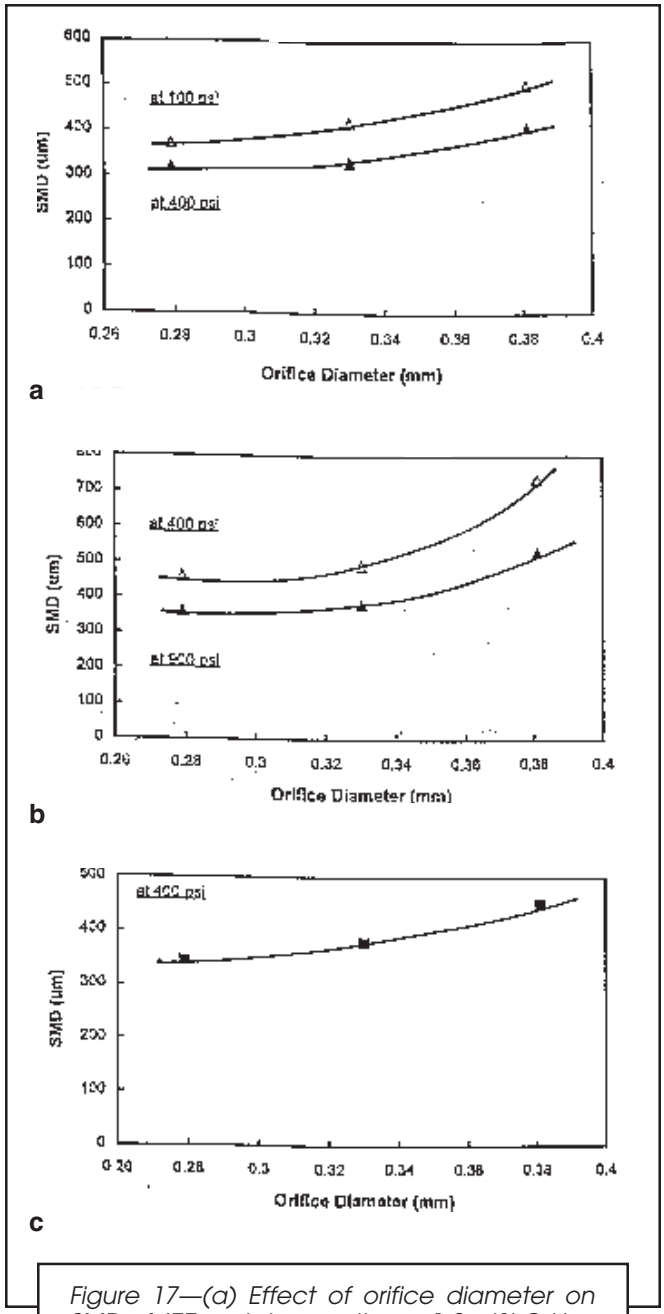

Figure 17—(a) Effect of orifice diameter on SMD of 477 nm latex coatings—1.0 wt% C_6H_{13}–HEUR. Symbols (Δ) at 100 psi; (▲) at 400 psi.
*(b) Effect of orifice diameter on SMD of 477 nm latex coatings—0.25 wt% HEC (mv = 9.5*10^5). Symbols (Δ) at 400 psi; (▲) at 900 psi.*
(c) Effect of orifice diameter on SMD of 68 nm latex coatings—1.7 wt% C_6H_{13}–HEUR and 400 psi.

with fan nozzles are predicted with good accuracy by the equation.

Concluding Remarks: In the 1976 study of Dorman and Stewart,[15] it was concluded that the spatter behavior of roll applied latex coatings was related to viscosities at high shear rates. This was an extremely limited study, and as in the case of defining a straight line on just two data points, deviations were not evident. In a four part series devoted to understanding the roll applications of coatings by the senior author of this contribution,[16] a detailed examination of commercial consumer latex paints provided clear evidence that roll spatter was not related to viscosities at high shear rates (HSVs). In a relatively recent presentation of these earlier studies to a major coatings research laboratory, the author was confronted in a very honest manner by one of the attendees: "You have not given us anything. It takes at least a day to measure an extensional viscosity, but I can measure on an ICI HSR "viscometer" HSVs within 30 seconds and I have management reports to write." Perhaps the current environment that emphasizes "depending on what the definition of is, is" is not the moment to consider the realities of an attempted scientific study.

The realities are that measurements of HSVs with an ICI "viscometer" is probably exceeded in depravity only by using a Ford cup for formulating an automotive coating for spray applications. It is well documented that in a cone and plate or parallel plate apparatus, the fluid fractures. Part of the fluid hangs with the boundary spinning at high velocity and part remains on the stationary plate. Then there is a problem of drying during a C/P measurement noted with two of the commercial latex coatings studied in the initial roll coating study. If these problems did not exist, the relatively low "high" shear rate from the ICI viscometer is nowhere near the deformation rate in most spray applications. One has to assume that the measurement is in the second Newtonian plateau region and therefore approximates the higher deformation rates in spray applications. The problems could be addressed by measuring shear viscosities at high shear rates in capillary viscometers, but pressures would have to be applied and such measurements would substantially exceed 30 sec.

The measurement and understanding of dynamic extensional viscosities is not in much better state-of-the-art condition. The extension rates are lower than occur in most spray applications, but at least the measurement is in the high deformation rate Newtonian region. There are other devices for measuring dynamic uniaxial extensional viscosities at higher extension rates, but they are far more time consuming than the device used in this study. Furthermore, the flow patterns from hollow and solid cone nozzles appear to be more complex,[12] involving biaxial or planar extensional flows. Measuring these types of viscosities on fluids is an unknown art at present. Progress is slow in this area.

SUMMARY

Dynamic uniaxial extensional viscosities of latex coatings dominate their airless spray patterns. Their shear viscosities and storage moduli do not significantly affect the atomization of spray sheets from non-Newtonian, latex coatings. In addition to DUEVs, the liquid pressure and orifice diameters influence spray droplet sizes, but the responses at high spray pressures are complicated by pulsation generated by higher turbulent flow of the fluids. A higher DUEV of the fluid helps delay the increase in turbulent flow of the fluid to higher pressures. Sauter mean diameters of droplet sizes in airless spray applications with fan nozzles are quantified with good

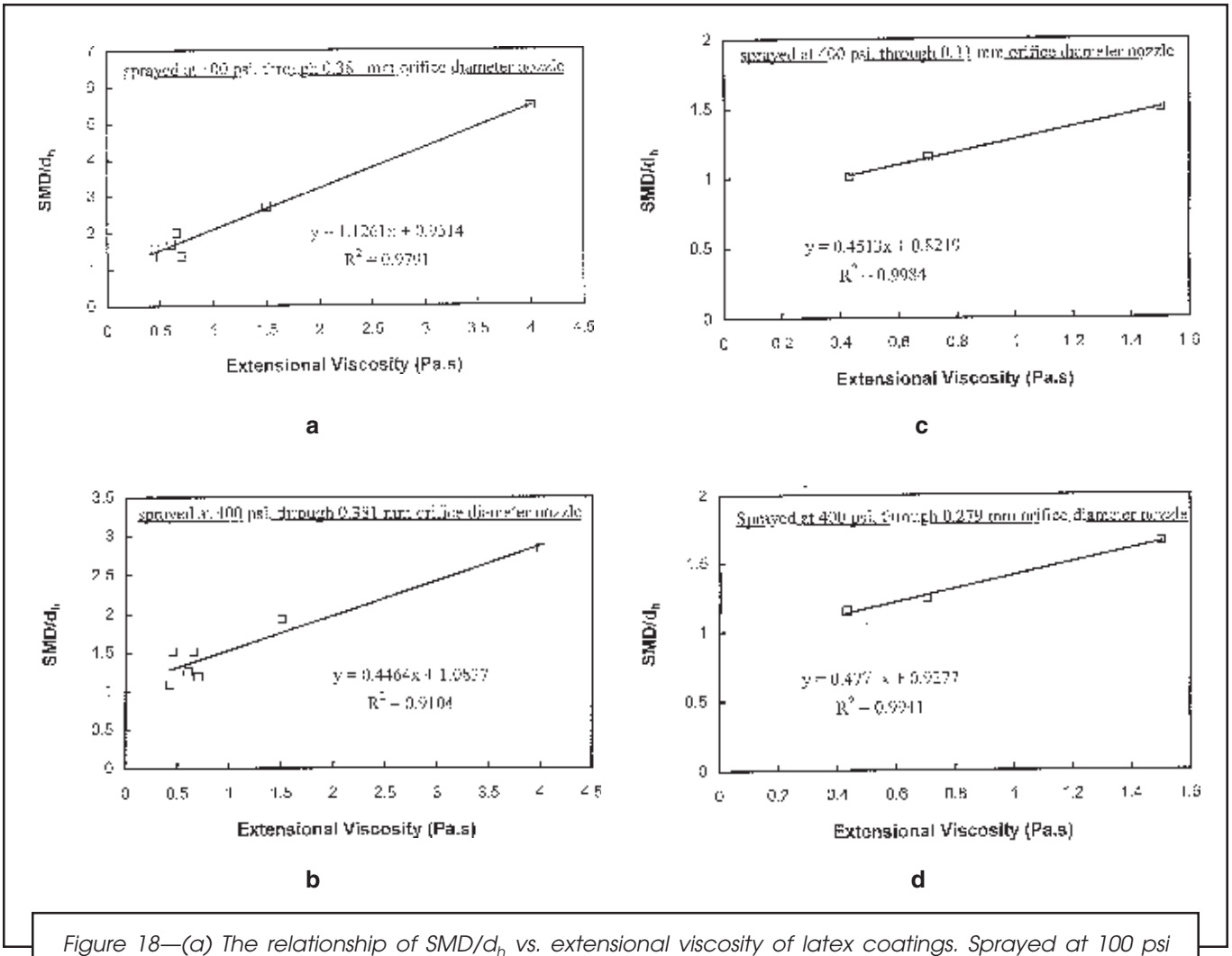

Figure 18—(a) The relationship of SMD/d_h vs. extensional viscosity of latex coatings. Sprayed at 100 psi through a fan nozzle with 0.381 mm orifice diameter.
(b) The relationship of SMD/d_h vs. extensional viscosity of latex coatings. Sprayed at 400 psi through a fan nozzle with 0.381 mm orifice diameter.
(c) The relationship of SMD/d_h vs. extensional viscosity of latex coatings. Sprayed at 400 psi through a fan nozzle with 0.33 mm orifice diameter.
(d) The relationship of SMD/d_h vs. extensional viscosity of latex coatings. Sprayed at 400 psi through a fan nozzle with 0.279 mm orifice diameter.

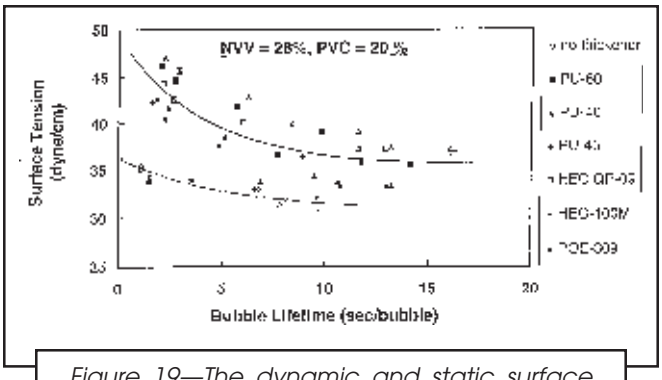

Figure 19—The dynamic and static surface tension of 477 nm latex coatings—different thickeners.

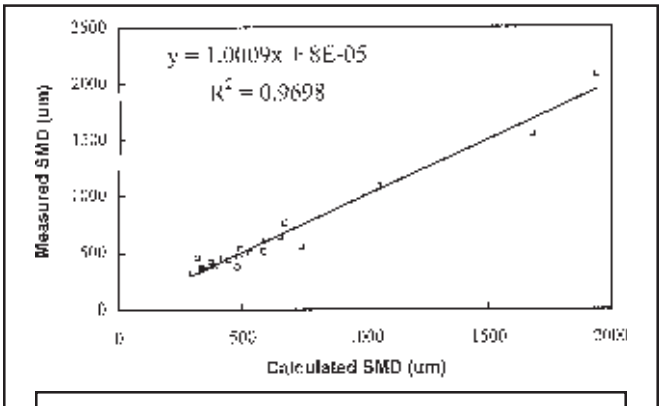

Figure 20—The calculated SMD vs. measured SMD of latex coatings—thickeners through airless spray process.

accuracy in this study, but this analysis applies only for the following experimental conditions due to the complexities involved in pulsations of the fluid discussed previously:

- dynamic uniaxial extensional viscosity of fluids: 0.4 ~ 4 Pa.s
- nozzle injection pressure: 100 ~ 1000 psi
- orifice diameter: 0.279 ~ 0.381 mm

ACKNOWLEDGMENT

The authors gratefully acknowledge the financial support of the National Science Foundation Industry/University Cooperative Research Center in Coatings at North Dakota State University.

References

(1) Levinson, S.B., "Application of Paint and Coatings," *Federation Series on Coatings Technology*, Federation of Societies for Coatings Technology, Philadelphia, PA, 1988.
(2) McBane, B.N., "Automotive Coatings," *Federation Series on Coatings Technology*, Federation of Societies for Coatings Technology, Philadelphia, PA, 1987.
(3) Zink, S.C., in *Encyclopedia of Chemical Technology*, 3rd Ed., Vol. 6, p. 414, 466, 1983.
(4) Rayleigh, L., *The Theory of Sound*, Vol. 2, Dover Publications, New York, (republication of 1896 edn.), pp. 343-75, 1945.
(5) Weber, C., *Z. Angew. Math. Mech.*, 11 (2), 136 (1931).
(6) Masters, K., *Spray Drying, An Introduction to Principles, Operational Practice and Applications*, 2nd Ed., John Wiley & Sons, New York, 1976.
(7) Snyder, H.E., Senser, D.W., and Lefebvre, A.H., *ASME J. Fluids Engineering*, 111, 342 (1989).
(8) Snyder, H.E., Senser, D.W., and Lefebvre, A.H., *IEE Transactions on Industry Applications*, 25 (4), 720 (1989).
(9) Lefebvre, A.H. and Senser, D.W., *Industrial Finishing* (June 16, 1990).
(10) Corbeels, P.L., Senser, D.W., and Lefebvre, A.H., *Atomization and Sprays*, 2, 87 (1992).
(11) Wang, X.F. and Lefebvre, A.H., *J. Propulsion*, 3 (1), 11 (1987).
(12) Xing, Lin-lin, Glass, J.E., and Fernando, R.H., in *Technology for Waterborne Coatings*, ACS Symposium Series 633, Glass, J.E. (Ed.), American Chemical Society, Washington, D.C., Chapter 15, 1997.
(13) Plla, S., *J. Oil & Colour Chemists' Assoc.*, 56, 195 (1973).
(14) Ginsberg, T., *FATIPEC*, 497-502, 1974.
(15) Dorman, J.D. and Stewart, D.M.D., *J. Oil Col. Chem. Assoc.*, 59, 115 (1976).
(16) Glass, J.E., "Dynamics of Roll Spatter and Tracking Part III: Importance of Extensional Viscosities," JOURNAL OF COATINGS TECHNOLOGY, *50*, No. 641, 56 (1978).
(17) Fernando, R.H. and Glass, J.E., *J. Rheology*, 32 (2), 199 (1988).
(18) Strivens, T.A., in *Paint and Surface Coatings, Theory and Practice*, Lambourne, R. (Ed.), Ellis Horwood Limited Publishers, Chichester, England, Chapter 15, 1988.
(19) Ming-Ren Tarng, M.R., Ma, Z., Alahapperuma, K., and Glass, J.E., in *Hydrophilic Polymers: Performance with Environmental Acceptability*, Advances in Chemistry Series 248, Glass, J.E. (Ed.), American Chemical Society, Washington, D.C., Chapter 24, 1996.
(20) Master, K., *Spray Drying, An Introduction to Principles, Operational Practice and Application*, 2nd Ed., John Wiley & Sons Inc., New York, 1976.
(21) Karunasena, A. and Glass, J.E., *Proc. ACS Div. Polymer Materials: Sci. Engin.*, 56, 627 (1987).
(22) Wang, S.Q., Drda, P.A., and Inn, Y.W., *J. Rheol.*, 40 (5), 875 (1996).
(23) Elliott, P.T., Ph.D. dissertation, North Dakota State University, in progress.